81-#5-80.

AIRBORNE ELECTROMAGNETIC SURVEY

ST. JOSEPH EXPLORATIONS LIMITED

RED AREA, BRITISH COLUMBIA

PROJECT #22092 MAY 9, 1981

Red Area: Red/1 (20 units)

Liard Mining Division: N.T.S. Location 94M-4

Latitude 59°00' to 59°07'
Longitude 127°45' to 128°00'

Owner and Operator of claims: St. Joseph Explorations Limited

Author: Dennis Kinvig

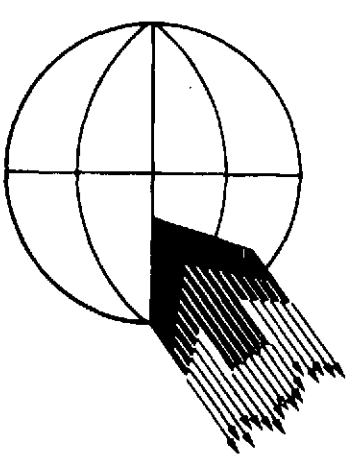

Questor Surveys Limited, 6380 Viscount Road, Mississauga, Ontario L4V 1H3

CONTENTS

INTRODUCTION

This report contains our interpretation of the results of an airborne electromagnetic survey flown in the Red Area of British Columbia, during January of 1981.

A brief description of the survey procedure together with recommendations for ground follow-up is included.

The total survey was 258 kilometers (161 miles) and the survey was performed by Questor Surveys Limited. The survey aircraft was a Shorts Skyvan C-FQSL and the operating base was Watson Lake, Yukon.

The area outline is shown on a 1:250,000 map at the end of this report. This is part of the National Topographic Series sheet number 94M.

FIELD CREW

Pilot	M. Portalier
Co-Pilot	B. Shields
Operator	B. Schieman
Engineer	P. Melen
Crew Manager	K. Cuomo

MAP COMPILATION

The base maps for navigation and flight path recovery were constructed from uncontrolled mosaics which were produced from photographs at a scale of 1:77,000. The final maps were reproduced at a scale of 1:15,000 on stable transparent film from which white prints can be made.

Flight path recovery was accomplished by comparison of the 35mm film with the mosaic in order to locate the fiducial points. These points were approximately 1145 meters apart.

SURVEY PROCEDURE

Terrain clearance was maintained as close to 122 meters as possible, with the E.M. Bird at approximately 46 meters above the ground. A recirculating flight path was used and the equipment operator logged the flight details and monitored the instruments.

The survey was flown with a mean line spacing of 400 meters.

INTERPRETATION AND RECOMMENDATIONS

The survey block is located about 90 kilometers southeast of Watson Lake, Yukon Territory. This is within the Rocky Mountain Thrust Belt near the Tintina Fault. The area is extensively covered with overburden of fluviatile and glacial origin, with outcrops occurring along the Red River. The mapped rock types include carbonaceous shale with some limestone, calcareous shale, sandstone, and orthoquartzite.

The survey area lies in a 'lead-zinc belt', with the town of Field marking the southern limit, and with Keno Hill marking the north end of the belt. Many of the deposits in this belt (e.g. - Vangorda Creek), in addition to containing galena, sphalerite, and silver, may occur with pyrrhotite, pyrite, and arsenopyrite in narrow fault veins and fractures, and along bedding planes.

Sulphide mineralization of this type should be detected by the INPUT method if the overburden is not too conductive. The conductivity is proportional to the amount of sulphides and/or graphitic material present. Most of the stronger conductors intercepted are thought to be associated with graphitic bearing shear zones and/or graphite shale layers. Possible targets should not be restricted to the

graphitic zones however, as other models for lead-zinc mineralization do exist (Mississippi Valley Type). The geology isn't known well enough to assume that only one model can exist.

Most of the three-channel and some of the four channel responses which display rapid decay rates are due to conductive overburden. During the course of the survey, an attempt was made to fly the flight lines in alternate directions. This procedure aids in the interpretation of a dip of a conductor. In some cases the channel peaks are staggered either in the direction of flight or in the opposite direction. This is an indication that the INPUT system is "seeing" a gently dipping conductive sheet, and the stagger is an indication of the direction of dip.

In order to simplify the INPUT maps, no attempt was made to put in all the conductor axes. The approach used was to divide the survey area into zones of conductivity and resistivity, and then relate these zones to the geology. An area is considered resistive even if it may have three-channel responses.

A brief discussion on the Red Area follows.

Red Area

The local geology is known from exposures found along the Red River. The beds have been folded into several overturned synclines and an anticline, all plunging to the south. There are several mineral occurrences. The anticlinal axis can be interpolated to pass through conductive Zone A, which corresponds to the carbonaceous and siliceous shale units. A geochemistry sample assaying at 510 ppm Pb and 26 ppm Ag was collected in this zone. The younger orthoquartzite appears to coincide with resistive Zone B.

There is a Pb-Zn occurrence in the sandstone/orthoquartzite. The recommendation that Zone B be considered an exploration target cannot be made without more knowledge on the type of mineralization present and what model it would fit. It is possible that the orthoquartzite may form a trap for upward moving metal-bearing fluids. If this is the case, the more promising exploration targets would be the flanks and apex of the anticline in Zone A (the shale unit).

Intercept 20780C - This three-channel anomaly lies over a small wedge of carbonaceous and calcareous shale bounded by several faults. The response is weak, and is probably due to the high conductivity contrast between the shale and the orthoquartzite.

Intercepts 20760E, 20760FX, 20751GG - They have moderate responses, stronger than most in Zone A, with 20760E having a depth estimate in excess of 60 meters. There is a Cu occurrence nearby.

Intercept 20790Z - This five-channel anomaly has a moderate response, and it has a depth estimate of 27 meters. It is located near the above mentioned geochemistry sample location. The conductivity may be partially due to the swamp.

It is proposed that any future ground reconnaissance survey (geochemistry, I.P.) should cover conductive Zone A in its entirely.

There are several responses with very high conductivities in the remainder of the area, which are thought to be due to graphitic shales. It has been suggested that there may be an association of lead-zinc mineralization with graphitic sediments. Perhaps intercept 20710F (74 siemens, depth estimate of 55 meters) as well as intercepts 20720E and F, 20760H, and others with relatively high conductivity, can be considered in any future project.

Dennis Kinvig

Dennis Kinvig,
Geologist.

APPENDIX

EQUIPMENT

The aircraft is equipped with a Mark VI INPUT (R) airborne E.M. system and Sonotek P.M.H. 5010 Proton Magnetometer. Radar altimeters are used for vertical control. The outputs of these instruments together with fiducial timing marks are recorded by means of galvanometer type recorders using light sensitive paper. Thirty-five millimeter continuous strip cameras are used to record the actual flight path.

(I) BARRINGER/QUESTOR MARK VI INPUT (R) SYSTEM

The Induced Pulse Transient (INPUT) system is particularly well suited to the problems of overburden penetration. Currents are induced into the ground by means of a pulsed primary electromagnetic field which is generated in a transmitting loop around the aircraft. By using half sine wave current pulses and a loop of large turns-area, the high output power needed for deep penetration is achieved.

The induced current in a conductor produces a secondary electromagnetic field which is detected and measured after the termination of each primary pulse. Detection is accomplished by means of a receiving coil towed behind the aircraft on four hundred feet of cable,

and the received signal is processed and recorded by equipment in the aircraft. Since the measurements are in the time domain rather than the frequency domain common to continuous wave systems, interference effects of the primary transmitted field are eliminated. The secondary field is in the form of a decaying voltage transient originating in time at the termination of the transmitted pulse. The amplitude of the transient is, of course, proportional to the amount of current induced into the conductor and, in turn, this current is proportional to the dimensions, the conductivity and the depth beneath the aircraft.

The rate of decay of the transient is inversely proportional to conductivity. By sampling the decay curve at six different time intervals, and recording the amplitude of each sample, an estimate of the relative conductivity can be obtained. By this means, it is possible to discriminate between the effects due to conductive near-surface materials such as swamps and lake bottom silts, and those due to genuine bedrock sources. The transients due to strong conductors such as sulphides exhibit long decay curves and are therefore commonly recorded on all six channels. Sheet-like surface materials, on the other hand, have short decay curves and will normally only show a response in the first two or three channels.

The samples, or gates, are positioned at 310, 490, 760, 1120, 1570 and 2110 micro-seconds after the cessation of the pulse. The widths of the gates are 180, 180, 360, 360, 540, and 540 micro-seconds respectively.

For homogeneous conditions, the transient decay will be exponential and the time constant of decay is equal to the time difference at two successive sampling points divided by the log ratio of the amplitudes at these points.

(II) SONOTEK P.M.H. 5010 PROTON MAGNETOMETER

The magnetometers which measure the total magnetic field have a sensitivity of 1 gamma and a range from 20,000 gammas to 100,000 gammas.

Because of the high intensity field produced by the INPUT transmitter, the magnetometer results are recorded on a time-sharing basis. The magnetometer head is energized while the transmitter is on, but the read-out is obtained during a short period when the transmitter is off. Using this technique, the head is energized for 0.83 seconds while the precession frequency is being recorded and converted to gammas. Thus a magnetic reading is taken every 1.13 second.

For this survey, a lag factor has been applied to the data. Magnetic data recorded on the analogue records at fiducial 10.00 for example would be plotted at fiducial 9.95 on the mosaics.

DATA PRESENTATION

The symbols used to designate the anomalies are shown in the legend on each map sheet, and the anomalies on each line are lettered in alphabetical order in the direction of flight. Their locations are plotted with reference to the fiducial numbers on the analog record.

A sample record is included to indicate the method used for correcting the position of the E.M. Bird and to identify the parameters that are recorded.

All the anomaly locations, magnetic correlations, conductivity-thickness values and the amplitudes of channel number 2 are listed on the data sheets accompanying the final maps.

GENERAL INTERPRETATION

The INPUT system will respond to conductive overburden and near-surface horizontal conducting layers in addition to bedrock conductors. Differentiation is based on the rate of transient decay, magnetic correlation and the anomaly shape together with the conductor pattern and topography.

Power lines sometimes produce spurious anomalies but these can be identified by reference to the monitor channel.

Railroad and pipeline responses are recognized by studying the film strips.

Graphite or carbonaceous material exhibits a wide range of conductivity. When long conductors without magnetic correlation are located on or parallel to known faults or photographic linears, graphite is most likely the cause.

Contact zones can often be predicted when anomaly trends coincide with the lines of maximum gradient along a flanking magnetic anomaly. It is unfortunate that graphite can also occur as relatively short conductors and produce attractive looking anomalies. With no other information than the airborne results, these must be examined on the ground.

Serpentinized peridotites often produce anomalies with a character that is fairly easy to recognize. The conductivity which is probably caused in part by magnetite, is fairly low so that the anomalies often have fairly large response on channel #1; they decay rapidly, and they have strong magnetic correlation. INPUT E.M. anomalies over massive magnetites show a relationship to the total Fe content. Below 25 - 30%, very little or no response at all is obtained, but as the percentage increases the anomalies become quite strong with a characteristic rate of decay which is usually greater than that produced by massive sulphides.

Commercial sulphide ore bodies are rare, and those that respond to airborne survey methods usually have medium to high conductivity. Limited lateral dimensions are to be expected and many have magnetic correlation caused by magnetite or pyrrhotite. Provided that the ore bodies do not occur within formational conductive zones as mentioned above, the anomalies caused by them will usually be recognized on an E.M. map as priority targets.

ITEMIZED COST STATEMENT

The Survey was conducted from January 10 to 12; three days; Questor INPUT Survey; 258 Line Kilometres at $31.69/ Line Kilometre = $8,176.02.

There was also a mobilization/demobilization fee of $1,000.00, for a TOTAL COST of $9,176.02.

Cost of preparation of the report is included in this figure.

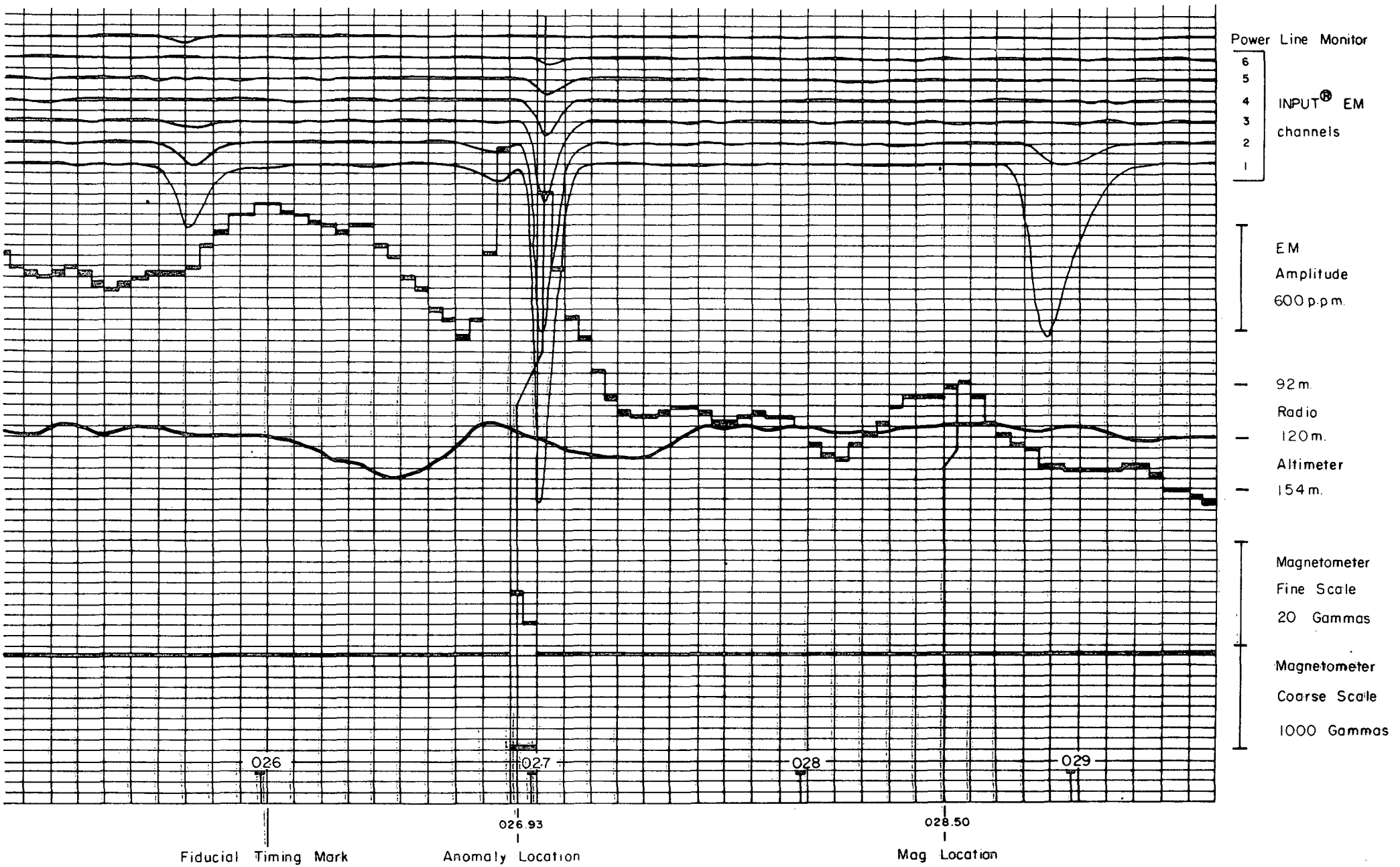

Representative INPUT®, Magnetometer and Altimeter Recording

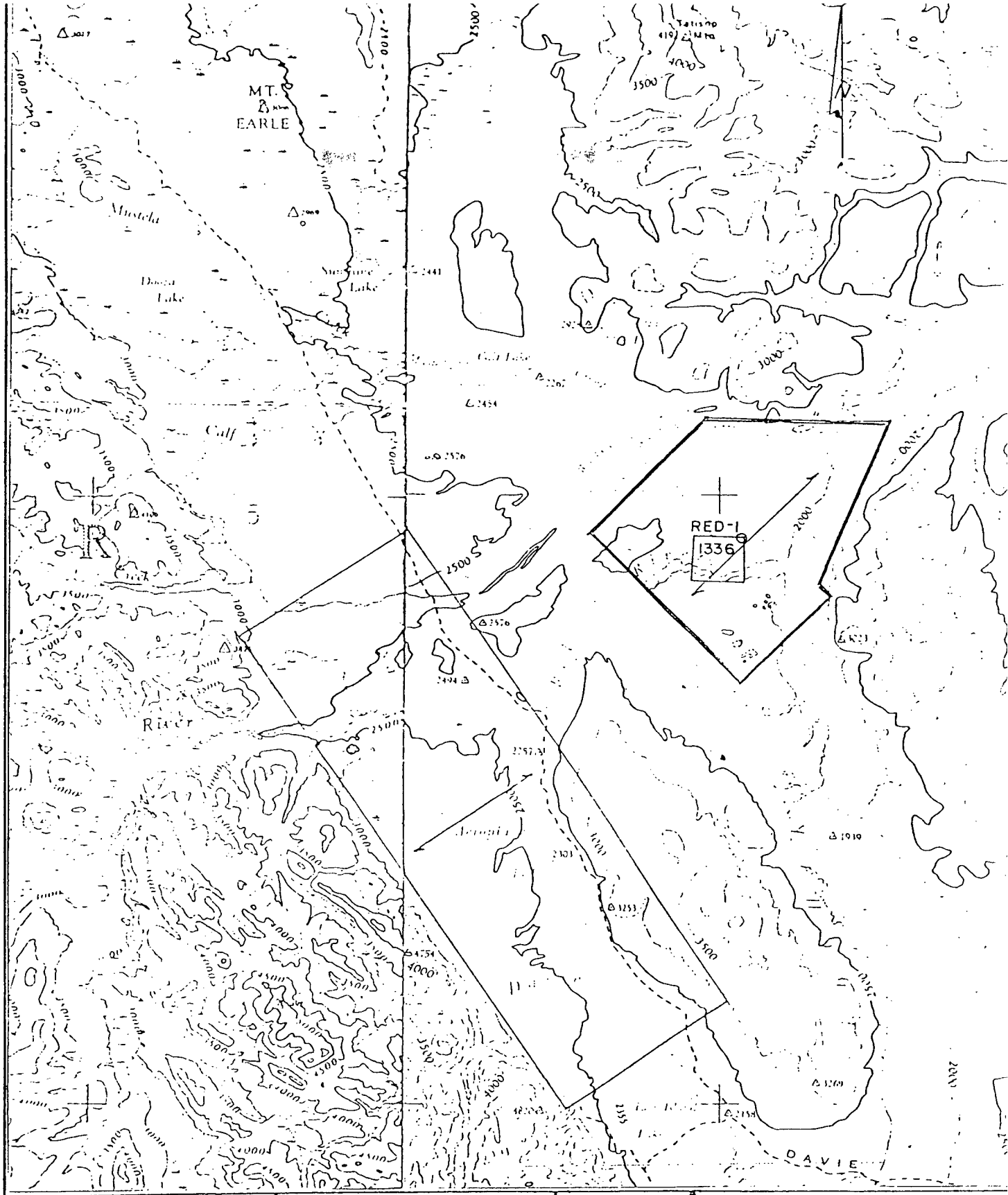

APPROX. LAT. & LONG. OF LOWER RT. COR. OF DWG. 59 ° 07 ' 00 " LATITUDE 127 ° 35 ' 00 " LONGITUDE	PROJECT NO. 5150.1 FIGURE NO.	SHEET NO. ____ OF ____ N.T.S. 94M	Scale: 1:250,000 2.5 0 25 5.0 7.5 km

ST. JOSEPH EXPLORATIONS LIMITED

TORONTO, CANADA

FINAL ANOMALY	FID	CHS	CH1.AMP	CH2.AMP	SIEMENS	MAG	VALUE
20660A	256.150	5		631	8	-	
20660B	256.900	4		397	2	-	
20660C	259.425	6		3230	10	-	
20670AX	228.800	4		900	4		
20670A	230.350	4		579	2	-	
20670B	230.950	3		341	1	-	
20670C	232.860	5		670	1		
20680A	233.225	5		509	5	-	
20680B	234.275	5		462	7	-	
20680C	235.325	5		384	27	-	
20680D	237.000	5		583	8	-	
20680E	237.425	5		752	9	-	
20680F	238.850	5		970	7	-	
20692A	171.625	6		786	6	-	
20692B	171.775	6		830	4	-	
20692C	172.075	4		430	1	-	
20692D	172.775	5		568	5	172.75	4
20692E	173.075	5		703	1	173.20	5
20692F	173.675	4		197	1	-	
20692G	174.225	4		166	3	174.10	7
20692H	174.775	6		757	31	-	
20692J	175.075	6		373	25	175.15	3
20692K	175.325	6		748	38	-	
20692L	175.775	4		279	4	175.70	4
20692M	176.400	5		445	4	-	
20701A	186.750	6		1330	4	-	
20701B	187.475	4		352	2	-	
20701C	187.750	5		686	3	187.65	3
20701D	188.000	6		865	4	-	
20701E	188.125	5		793	1	-	
20701F	188.400	4		274	1	188.40	4
20701G	188.700	5		428	3	-	
20701H	189.350	4		197	3	-	
20701J	190.550	6		797	43	-	
20701K	190.750	6		923	58	-	
20701L	190.900	4		719	15	191.25	9
20701M	191.700	6		1298	19	-	
20701N	192.025	6		3433	14	-	
20701P	192.150	6		3608	38	-	
20710A	221.250	6		947	12	-	
20710B	221.750	5		522	23	221.70	6
20710C	222.300	6		1337	30	-	
20710D	222.450	6		1268	23	-	
20710E	223.850	6		1021	51		

FINAL ANOMALY	FID	CHS	CH1.AMP	CH2.AMP	SIEMENS	MAG	VALUE
20710F	224.500	6		696	74	-	
20710G	226.025	5		299	1	-	
20710H	226.425	5		874	7	-	
20710J	226.775	5		1095	1	-	
20710K	227.825	5		601	1	-	
20710L	228.330	4		1420	1		
20720A	178.525	5		755	4	-	
20720B	178.800	5		1070	1	-	
20720C	180.000	5		1020	2	-	
20720D	180.675	5		461	5	-	
20720E	181.600	4		179	20		
20720F	182.900	6		2610	50	-	
20720G	183.050	6		1979	55	-	
20720H	183.250	6		1579	38	183.35	4
20720J	183.450	6		1907	39	-	
20720K	183.650	6		2507	27	-	
20720L	184.250	4		341	7		
20720M	185.175	6		547	14	-	
20732A	176.850	6		820	8	-	
20732B	177.050	6		599	20	-	
20732C	177.225	4		464	5		
20732D	177.725	6		615	18	177.50	5
20732E	178.100	6		724	63	-	
20732F	178.500	6		1893	53	-	
20732G	178.725	6		3003	22	-	
20732H	178.850	6		3369	23	-	
20732J	179.000	4		2147	17		
20732K	180.150	6		2347	33	-	
20732L	180.300	6		1735	42	-	
20732M	180.550	6		1060	51	-	
20732N	181.150	6		1936	36	-	
20732P	181.400	6		2998	22	-	
20732R	181.600	6		1961	22		
20732S	183.875	3		531	1	-	
20732T	184.300	4		656	1	184.30	3
20732W	185.075	4		435	2	185.10	3
20732Y	185.400	4		360	5	-	
20732Z	185.675	4		491	2	-	
20732AA	186.100	5		657	1	-	
20740A	158.325	4		616	3	-	
20740B	159.575	5		979	3	-	
20740C	160.250	4		822	1	-	
20740D	162.200	6		1175	34		
20740E	162.625	6		3003	43	-	
20740F	162.875	6		2865	44	-	
20740G	163.225	6		1621	28	-	
20740H	163.700	6		1181	24	-	
20740J	164.300	6		1646	50	-	
20740K	164.700	6		4160	36		

FINAL ANOMALY	FID	CHS	CH1.AMP	CH2.AMP	SIEMENS	MAG	VALUE
20740L	164.900	6		5912	24	-	
20740M	165.275	6		4080	53	-	
20740N	165.550	6		3074	40	-	
20740P	165.800	6		1749	34	-	
20740R	166.000	6		1349	27	-	
20740S	166.550	6		592	25	-	
20740T	166.825	6		896	7		
20751A	192.675	6		1961	19	-	
20751B	193.000	6		1640	8	192.85	3
20751C	193.150	6		1633	19	-	
20751D	193.550	3		474	1	193.75	3
20751E	194.000	3		556	1	-	
20751F	194.300	6		637	16	194.35	3
20751G	194.700	6		853	15	-	
20751H	194.900	6		2753	22	-	
20751J	195.025	6		3144	29	-	
20751K	195.325	6		1769	14	-	
20751L	195.600	6		1269	34	-	
20751M	195.925	6		1013	35	-	
20751N	196.250	6		1970	30	-	
20751P	196.400	6		1773	35	-	
20751R	196.775	6		1601	44	-	
20751S	196.925	6		1386	41	-	
20751T	197.175	6		926	41	-	
20751W	197.625	6		1458	46	-	
20751Y	197.850	6		1517	37	-	
20751Z	198.100	6		1693	39	-	
20751AA	198.500	6		1946	48	-	
20751BB	198.650	6		2343	39	198.70	4
20751CC	198.825	6		2393	41	-	
20751DD	199.050	6		1934	55	-	
20751EE	199.175	6		1646	41	-	
20751FF	199.450	5		665	16	-	
20751GG	201.300	4		448	1	-	
20751HH	201.625	4		379	3	-	
20751JJ	201.975	4		673	1	201.85	7
20751KK	202.175	5		736	2	202.35	3
20751LL	202.750	5		520	4	-	
20751MM	203.075	5		680	7	203.05	3
20751NN	203.400	4		321	1	-	
20760A	137.000	5		281	17	-	
20760B	137.375	5		525	4	-	
20760C	137.775	5		691	2	-	
20760D	138.075	4		653	1	138.30	3
20760E	138.750	5		522	3	-	
20760F	140.500	6		502	23	-	
20760G	140.725	6		1277	35	-	
20760H	140.875	6		2296	53	-	
20760J	141.000	6		3080	41	-	
20760K	141.175	6		2480	46	-	
20760L	141.425	6		2260	37		

FINAL ANOMALY	FID	CHS	CH1.AMP	CH2.AMP	SIEMENS	MAG	VALUE
20760M	141.675	6		2183	30		
20760N	141.925	6		2258	36	–	
20760P	142.225	6		1711	21	–	
20760R	142.850	6		2183	42	–	
20760S	143.025	6		2405	43	–	
20760T	143.200	6		2695	36	–	
20760W	143.600	6		3995	38	–	
20760Y	143.875	6		4602	25	–	
20760Z	144.175	6		2173	43	–	
20760AA	144.450	6		1080	37	–	
20760BB	145.300	6		1770	26	–	
20760CC	145.525	6		1826	27	–	
20760DD	145.825	6		2598	5	–	
20760EE	146.475	6		3295	1	–	
20760FF	146.875	6		6366	5	–	
20760GG	147.250	6		4676	24	–	
20760HH	147.500	6		5038	4	–	
20760JJ	147.650	6		2907	5	–	
20770A	168.025	5		2480	8	–	
20770B	168.325	5		3058	7	–	
20770C	168.425	6		2908	13	–	
20770D	168.750	6		1086	7	–	
20770E	169.225	6		1004	13	–	
20770F	169.450	6		495	33	–	
20770G	169.800	6		1170	16	–	
20770H	170.000	6		2382	33	–	
20770J	170.475	6		976	58	–	
20770K	171.500	6		3697	42	–	
20770L	171.650	6		4725	49	–	
20770M	171.800	6		4041	28	–	
20770N	171.950	6		3529	28	–	
20770P	172.050	6		3978	24	–	
20770R	172.150	6		4063	28	–	
20770S	172.300	6		3541	29	–	
20770T	172.475	6		2022	26	–	
20770W	172.700	6		4166	26	–	
20770Y	172.800	6		4319	15	–	
20770Z	172.950	6		2903	19	–	
20770AA	173.550	6		2825	29	–	
20770BB	173.925	6		2031	41	–	
20770CC	175.475	5		803	3	–	
20770DD	176.000	5		352	5	–	
20770EE	176.870	4		660	2	–	
20770FF	177.275	5		627	3	–	
20770GG	177.775	6		564	7		
20780A	116.100	4		403	5	–	
20780B	116.675	5		1077	2	–	
20780C	117.700	3		346	1	–	
20780D	118.500	4		855	1	–	
20780E	120.250	6		2864	27	–	
20780F	120.650	6		5676	12	–	

FINAL ANOMALY	FID	CHS	CH1.AMP	CH2.AMP	SIEMENS	MAG	VALUE
20780G	120.900	6		5092	28		
20780H	121.225	6		2817	35	121.10	3
20780J	121.475	6		3351	24	--	
20780K	121.750	6		2754	36		
20780L	122.700	6		1485	29	122.60	3
20780M	123.250	5		363	36	--	
20780N	123.850	6		1235	15	--	
20780P	124.000	6		1469	22	--	
20780R	124.350	6		2019	21	--	
20780S	124.625	6		1785	15	--	
20780T	124.925	6		969	45	--	
20780W	125.150	6		1306	20	--	
20780Y	125.425	5		544	4	--	
20780Z	125.850	6		694	12	--	
20780AA	126.150	6		1303	23		
20790A	148.100	6		1629	26	--	
20790B	148.300	6		1704	15	--	
20790C	148.575	6		1619	4	--	
20790D	148.875	6		3500	13	--	
20790E	149.200	6		1031	29	--	
20790F	149.600	6		963	21	--	
20790G	149.825	6		1597	21		
20790H	149.950	6		1153	15	--	
20790J	150.125	6		891	14	--	
20790K	150.700	6		625	54	--	
20790L	151.225	6		1371	36	--	
20790M	151.300	6		1640	24	--	
20790N	152.125	6		5868	21		
20790P	152.450	6		3465	25	--	
20790R	152.575	6		3224	26	--	
20790S	152.700	6		3349	38	--	
20790T	152.900	6		3587	44	--	
20790W	153.100	6		2949	24	153.15	3
20790Y	153.325	6		2812	30	153.40	4
20790Z	155.000	5		1011	3	--	
20790AA	155.375	4		605	1	--	
20790BB	156.375	4		608	1	--	
20790CC	156.775	4		564	1	--	
20790DD	157.300	4		536	2	--	
20800A	82.325	5		635	3	82.45	2
20800B	82.875	4		467	1	--	
20800C	83.050	4		448	1	--	
20800D	83.750	4		517	4	--	
20800E	84.325	4		1608	1		
20800F	84.475	4		1530	1	--	
20800G	85.025	4		402	1	--	
20800H	86.000	6		1328	23	--	
20800J	86.600	6		3031	33	--	
20800K	86.875	6		3247	21	--	
20800L	87.125	6		3994	23		

FINAL ANOMALY	FID	CHS	CH1.AMP	CH2.AMP	SIEMENS	MAG	VALUE
20800M	87.350	6		3532	17		
20800N	87.775	6		1407	27	–	
20800P	87.900	6		1394	25	–	
20800R	88.100	6		1235	23	–	
20800S	88.225	6		1388	38	88.40	6
20800T	88.875	6		604	37	–	
20800W	89.425	6		1061	26	–	
20800Y	89.500	6		1054	23	–	
20800Z	89.900	4		1005	2	–	
20800AA	90.100	6		1764	25	–	
20800BB	90.500	6		2011	41	90.50	3
20810A	126.525	6		1681	49	–	
20810B	126.750	6		2153	26	–	
20810C	127.050	6		2603	32	–	
20810D	127.225	6		2247	32	–	
20810E	127.525	6		1568	11	–	
20810F	127.850	6		1096	16		
20810G	128.025	6		1049	50	–	
20810H	128.275	6		640	48	–	
20810J	128.700	5		487	59	–	
20810K	129.175	6		1334	36	129.15	5
20810L	129.425	6		2768	31	–	
20810M	129.550	6		3440	20		
20810N	129.650	6		3124	20	–	
20810P	129.925	6		4208	11	–	
20810R	130.325	6		3005	31	–	
20810S	130.750	6		4071	28	–	
20810T	131.350	6		1164	18	–	
20810W	131.500	6		1367	20		
20810Y	132.450	4		1439	1	–	
20810Z	133.250	4		482	2	–	
20810ZX	132.600	5		1340	1	–	
20810AA	134.600	5		888	2	–	
20810BB	135.150	4		516	2		
20820A	64.900	5		721	3	–	
20820B	65.425	4		1337	1	–	
20820C	65.650	4		743	2	–	
20820D	66.025	4		647	1	–	
20820E	66.750	4		375	1	–	
20820F	67.000	3		585	1		
20820G	68.500	6		1495	30	–	
20820H	68.700	6		1804	11	–	
20820J	69.725	6		1111	25	–	
20820K	69.975	6		3305	12	–	
20820L	70.225	6		2324	25	–	
20820M	70.400	6		2914	39	–	
20820N	71.100	6		677	35	–	
20820P	71.400	6		555	28	–	
20820R	71.825	6		674	34	–	
20820S	72.300	6		1609	37	–	
20820T	72.625	6		1540	37	–	
20820W	73.700	6		1625	18		

FINAL ANOMALY	FID	CHS	CH1.AMP	CH2.AMP	SIEMENS	MAG	VALUE
20830A	91.225	6		2993	19		
20830B	91.400	6		2315	19	--	
20830C	91.550	6		2534	32	--	
20830D	91.925	6		1077	36	--	
20830E	92.400	6		1128	33	--	
20830F	92.725	6		822	35	--	
20830G	93.050	6		1059	23		
20830H	93.300	6		1687	8	--	
20830J	93.550	6		2316	11	--	
20830K	93.800	6		2438	30	--	
20830L	94.150	6		963	16	--	
20830M	95.175	6		1826	16	--	
20830N	95.375	6		1298	19	--	
20830P	95.650	6		1026	16	--	
20830R	96.390	3		500	1	--	
20830S	98.650	4		606	1	--	
20840A	47.900	4		557	3	--	
20840B	48.200	4		513	2	--	
20840C	48.800	5		820	3	--	
20840D	49.400	4		629	1	--	
20840E	51.850	6		560	60		
20840F	52.400	6		6443	26	--	
20840G	52.625	6		5284	15	--	
20840H	52.825	6		2219	35	--	
20840J	53.400	6		2438	7	--	
20840K	53.525	6		2269	6	--	
20840L	53.825	6		1720	17		
20840M	54.300	6		704	8	--	
20840N	54.650	6		835	26	--	
20840P	55.100	6		1048	32	--	
20840R	55.875	6		3232	34	--	
20850A	73.750	6		585	24	--	
20850B	74.175	6		635	5	--	
20850C	74.350	6		857	8	--	
20850D	74.550	6		813	12	--	
20850E	74.900	6		985	16	--	
20850F	75.125	6		1866	22	--	
20850G	75.475	6		1635	8	--	
20850H	75.875	6		6454	27	--	
20850J	76.100	6		5039	16	--	
20850K	76.225	6		4173	25	--	
20850L	76.375	6		5255	22	--	
20850M	76.775	6		3677	9		
20850N	79.375	5		672	2	--	
20850P	79.975	6		891	9	--	
20850R	80.125	6		950	7	--	
20850S	80.900	5		466	2	--	

FINAL ANOMALY	FID	CHS	CH1.AMP	CH2.AMP	SIEMENS	MAG	VALUE
20860AX	35.020	4		900	1		
20860A	37.800	6		3087	7		
20860B	38.200	6		2455	11	-	
20860C	38.850	6		2118	6	-	
20860D	39.250	6		2222	21	-	
20860E	39.850	6		922	15	-	
20860F	40.350	6		881	17	-	
20870A	56.800	6		752	5	-	
20870B	57.150	6		611	27	-	
20870C	57.575	6		1999	36	-	
20870D	57.775	6		2790	28	-	
20870E	57.950	6		2283	19	-	
20870F	58.225	6		3452	7	-	
20870G	58.425	6		2690	7	-	
20870H	58.600	6		2512	10	-	
20870J	59.000	6		1993	14	-	
20870K	61.475	5		844	6	-	
20870L	61.975	5		673	9	-	
20870M	62.675	5		779	2	-	
20881A	18.625	4		393	1	-	
20881B	19.425	5		528	3	19.25	3
20881C	19.800	6		887	8	19.70	3
20881D	20.100	6		725	11	-	
20881E	20.800	5		941	8	-	
20881F	21.000	6		910	7	-	
20881G	21.225	5		873	4	-	
20881H	23.250	5		914	3	-	
20881J	23.675	6		4386	15	-	
20881K	24.300	6		4643	39	-	
20881L	24.400	6		4905	33	-	
20881M	24.600	6		4458	36	-	
20881N	25.325	6		584	49	-	
20881P	25.525	6		828	22	25.50	3
20881R	25.800	6		331	14	25.80	3
20890A	41.200	5		435	22	-	
20890B	42.250	6		1485	11		
20890C	42.625	6		2842	41	-	
20890D	42.775	6		3245	34	-	
20890E	43.025	6		2389	29	-	
20890F	43.225	6		3258	20	-	
20890G	46.800	6		1084	5	-	
20890GX	44.950	4		930	1		
20890GY	45.830	4		1130	1		
20900A	26.700	6		341	21	-	
20900B	27.025	4		525	8	-	
20900C	27.350	6		1300	28	-	
20900D	27.600	6		913	11	-	
20900E	27.825	4		502	29		

FINAL ANOMALY	FID	CHS	CH1.AMP	CH2.AMP	SIEMENS	MAG	VALUE	
20900F	28.125	6		676	38	-		
20900G	28.500	4		751	6	-		
20900H	30.200	6		1149	5	-		
20900J	30.425	6		980	12			
20900K	31.250	4		927	4	-		
20900L	31.950	6		1106	9	-		
29030A	240.425	4		810	3	240.30	5	
29030B	241.775	4		401	1			
29030C	242.175	4		429	2	-		
29030D	244.750	4		819	1	-		
29030E	242.100	4		824	5	-		
29040A	249.450	5		464	9	-		
29040B	249.750	5		464	16	-		
29040C	250.300	6		627	60	-		
29040D	250.700	6		1511	30	N/P falls on 20820G		
29040E	251.000	6		2011	13	-		
29040F	252.775	6		1376	57	-		
29040G	252.925	6		1504	57	-		
29040H	253.050	6		1538	46	-		
29040J	253.125	6		1576	32	N/P falls on 20751EE		
29040K	253.450	6		2048	30	-		
29040L	253.550	6		2301	30	-		
29040M	253.675	6		2379	33	-		
29040N	253.850	6		2673	28	-		
29040P	254.075	6		1651	40	-		
29040R	254.250	6		1219	42	-		
29040S	254.700	6		819	45			
29050A	259.900	6		540	7	259.85	4	
29050B	260.425	6		2099	19	-		
29050C	260.650	6		1314	19	-		
29050D	260.900	6		774	25	260.95	6	
29050E	261.100	6		796	44	-		
29050F	261.750	6		664	52	-		
29050G	261.875	6		714	48	-		
29050H	262.175	6		783	41	-		
29050J	262.250	6		792	32	-		
29050K	262.750	6		1330	46			
29050L	262.850	6		1433	46	-		
29050M	262.950	6		1586	33	-		
29050N	263.200	6		1401	28	-		
29050P	263.650	6		1245	31	-		
29050R	263.800	6		1232	48	-		
29051A	264.800	6		401	122	-		
29051B	265.000	6		504	34	-		
29051C	265.175	6		482	67	-		
29051D	265.925	6		879	65	-		
29051E	266.150	6		1167	50			

FINAL ANOMALY	FID	CHS	CH1.AMP	CH2.AMP	SIEMENS	MAG	VALUE
~~29051F~~	~~266.400~~	~~6~~		~~1288~~	~~27~~	~~-~~	
290516	267.025	6		2697	38	-	

$

ADDITIONS

20732BB	186.440	3		500	1	
20760FX	139.140	3		380	1	-
20820GX	67.630	3		690	1	
20900AX	26.180	6		980	21	

Legend

- 6 Channel Anomaly
- 5 Channel Anomaly
- 4 Channel Anomaly
- 3 Channel Anomaly
- 2 Channel Anomaly
- Magnetic Correlation

Anomaly Letter — B, 5 — Apparent Conductivity-Width
1800 — Ch. 2 Amplitude P.P.M.

Interpretation

Direction of Dip

Zone of Conductivity

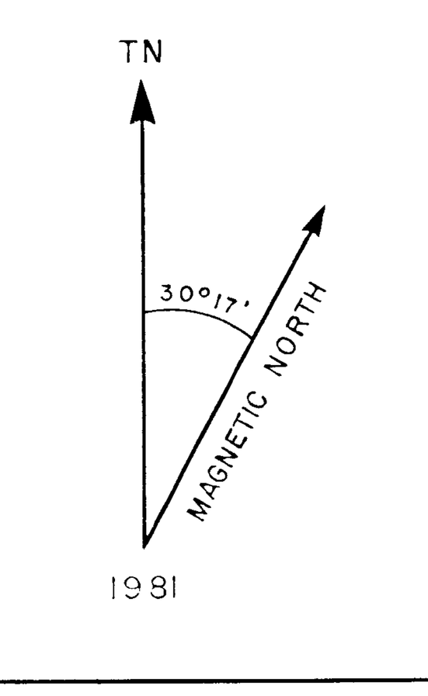

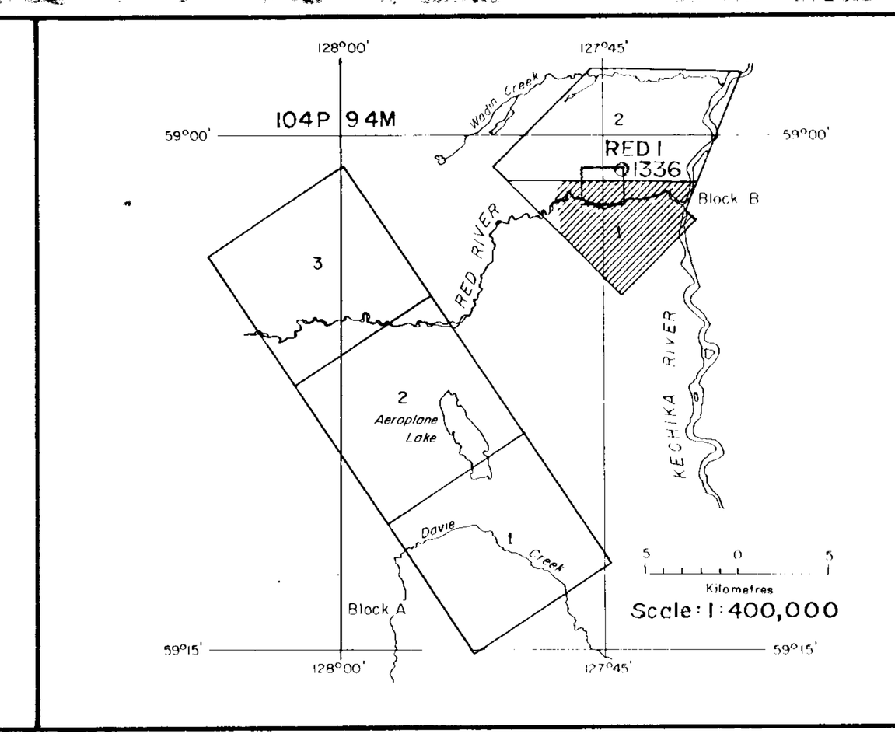

QUESTOR SURVEYS LIMITED

Airborne Mk VI Input Survey

RED AREA, B.C.

NTS 94 M

SCALE 1:15,000

Metres 300 0 300 600 900 Metres

Drawn By	Dataplotting
Dates Flown	January, 1981
Flight Path Recovery	D.G., S.H., B.D.P.
Data Reduction	R.D., W.K.
Completed	March, 1981
Checked	D.K.
File No. 22092 Blk. B	Map 1 of 2

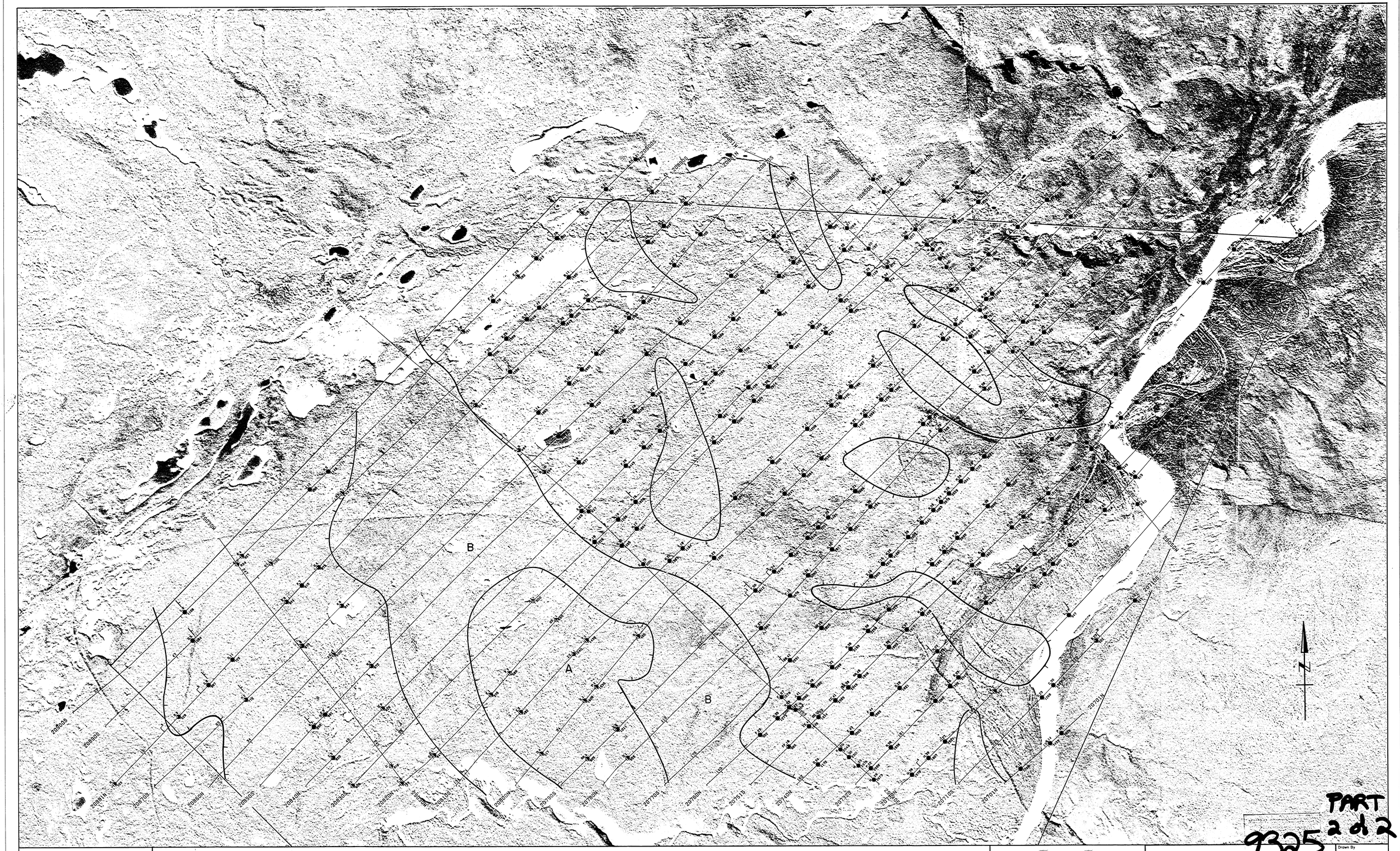

Legend

- 6 Channel Anomaly
- 5 Channel Anomaly
- 4 Channel Anomaly
- 3 Channel Anomaly
- 2 Channel Anomaly
- Magnetic Correlation

Anomaly Letter — B, 5 — 1800 — Apparent Conductivity-Width

Ch. 2 Amplitude P.P.M.

Interpretation

Direction of Dip

Zone of Conductivity

TN

30°17'

MAGNETIC NORTH

1981

104P 94M

Scale 1:400,000

QUESTOR SURVEYS LIMITED

Airborne Mk VI Input Survey

RED AREA, B.C.

NTS 94 M

SCALE 1:15,000

Metres 300 0 300 600 900 Metres

Drawn By	Dateplotting
Dates Flown	January, 1981
Flight Path Recovery	D.G., S.H., B.D.P.
Data Reduction	R.D., W.K.
Completed	March, 1981
Checked	D.K.
File No. 22092 Blk. B	Map 2 of 2

PART 2 of 2

9325